

# Molecular Orbitals Support Energy-Stabilizing ‘Bonding’ Nature of Bader’s Bond Paths

Ignacy Cukrowski,\* Jurgens H. de Lange, Daniël M. E. van Niekerk and Thomas G. Bates

*Department of Chemistry, Faculty of Natural and Agricultural Sciences, University of Pretoria,  
Lynnwood Road, Hatfield, Pretoria 0002, South Africa*

\*Correspondence to: Ignacy Cukrowski

E-mail: ignacy.cukrowski@up.ac.za

## ABSTRACT

Our MO-based findings proved a bonding nature of each density bridge (DB, or a bond path with an associated critical point, CP) on a Bader’s molecular graph. A DB pin-points universal physical and net energy-lowering processes that might, but do not have to, lead to a chemical bond formation. Physical processes leading to electron density (ED) concentration in inter-nuclear regions of three distinctively different homo-polar H,H atom-pairs as well as classical C–C and C–H covalent bonds were found to be *exactly the same*. Notably, properties of individual MOs are inter-nuclear-region specific as they (i) either concentrate, deplete or do not contribute to ED at a CP and (ii) delocalise electron-pairs through either in- (positive) or out-of-phase (negative) interference. Importantly, dominance of a net ED concentration and positive  $e^-$ -pairs delocalisation made by a number of  $\sigma$ -bonding MOs is a common feature at a CP. This feature was found for the covalently-bonded atoms as well as homo-polar H,H atom-pairs investigated. The latter refer to a DB-free H,H atom-pair of the bay in the twisted biphenyl (Bph) and DB-linked H,H atom-pairs (i) in cubic  $\text{Li}_4\text{H}_4$ , where each H-atom is involved in three highly repulsive interactions (over +80 kcal/mol) and (ii) involved in a weak attractive interaction when sterically clashing in the planar Bph.

# 1. INTRODUCTION

Chemistry is synonymous with the concept of chemical bonding that is being debated for decades with most approaches being solidly routed in two major ‘families’ of quantum mechanics (QM) methods. The first, wavefunction-based family encompasses applications of (i) molecular orbitals (MO),<sup>1-4</sup> valence bond (VB) theory,<sup>1,2,5,6</sup> natural bond orbital (NBO)<sup>7-9</sup> and natural orbitals for chemical valence (NOCV) within the ETS-NOCV<sup>10-13</sup> energy decomposition scheme (ETS = extended transition state). The second, electron density (ED) based family (the quantum chemical topology (QCT) methods) incorporates the quantum theory of atoms in molecules (QTAIM),<sup>14-16</sup> interacting quantum atoms (IQA),<sup>17-19</sup> fractional occupation iterative Hirshfeld (FOHI),<sup>20,21</sup> and fragment attributed molecular system energy change (FAMSEC).<sup>13,22-24</sup> Most methods within orbital and electron density based approaches have been successfully applied in describing chemical bonding for many decades. Even though the two families have QM as a common denominator, their interpretations of chemical bonding might be drastically different. A typical, but not exclusive, example is a ubiquitous<sup>25,26</sup> homopolar H,H atom-pair involved in a steric intra- and inter-molecular CH...HC contact in crowded molecular environments. To this effect, biphenyl (Bph) became an iconic subject of a nearly 3-decade long scientific debate.<sup>25-40</sup> This is because (i) Bader’s bond path (BP)<sup>14</sup> links *ortho*-H atoms that, according to the generally accepted view, are involved in a *steric repulsive interaction*<sup>27,30</sup> in planar Bph and (ii) one could computationally investigate (dis)appearance of a BP on rotating two phenyl rings. Moreover, Bph is a prototype molecule in numerous studies and it features, as a molecular core, in 2.6% of all Cambridge Structural Database (CSD) structures.<sup>41</sup>

Notably, it is not the appearance of a BP between *ortho*-H-atoms involved in a steric contact but its (non)bonding interpretation that became a subject of a battle between the two camps. To avoid unnecessary repetitions, readers interested in historic development of this research debate are referred to most recent paper by Popelier.<sup>39</sup> Briefly, Bader’s notion of a bond path

representing an interaction of a bonding nature is generally supported/rejected by researches entrenched in the QCT/wavefunction-based interpretations. As a matter of fact, the dispute on chemical interpretation of a BP extended to other and classically ‘unexpected’ appearances of BPs, such as between He and C-atoms of adamantane,<sup>42–44</sup> between noble gas atoms and noble gas and C atoms in endohedral fullerenes Ng<sub>2</sub>@C60 (Ng=He–Xe),<sup>45</sup> He, F, F<sup>-</sup> dimers<sup>46</sup> or water dimers,<sup>47</sup> bay-type H···H interaction in *cis*-2-butene,<sup>9,13,48</sup> or phenanthrene.<sup>25,40,49</sup>

Our main aim is to put forth a chemical interpretation of BPs by investigating physical processes leading to the absence or presence of a BP. Our focus is on individual canonical MOs’ nature and contribution made to the electron density in specific inter-nuclear regions. Two classical covalent, C–C and C–H, bonds in Bph, the bay-type steric CH···HC contact in the planar Bph, the CH···HC inter-nuclear region without a BP in the twisted Bph, and finally the H···H interactions in a cubic form of LiH (Li<sub>4</sub>H<sub>4</sub>) will be investigated - Figure 1.

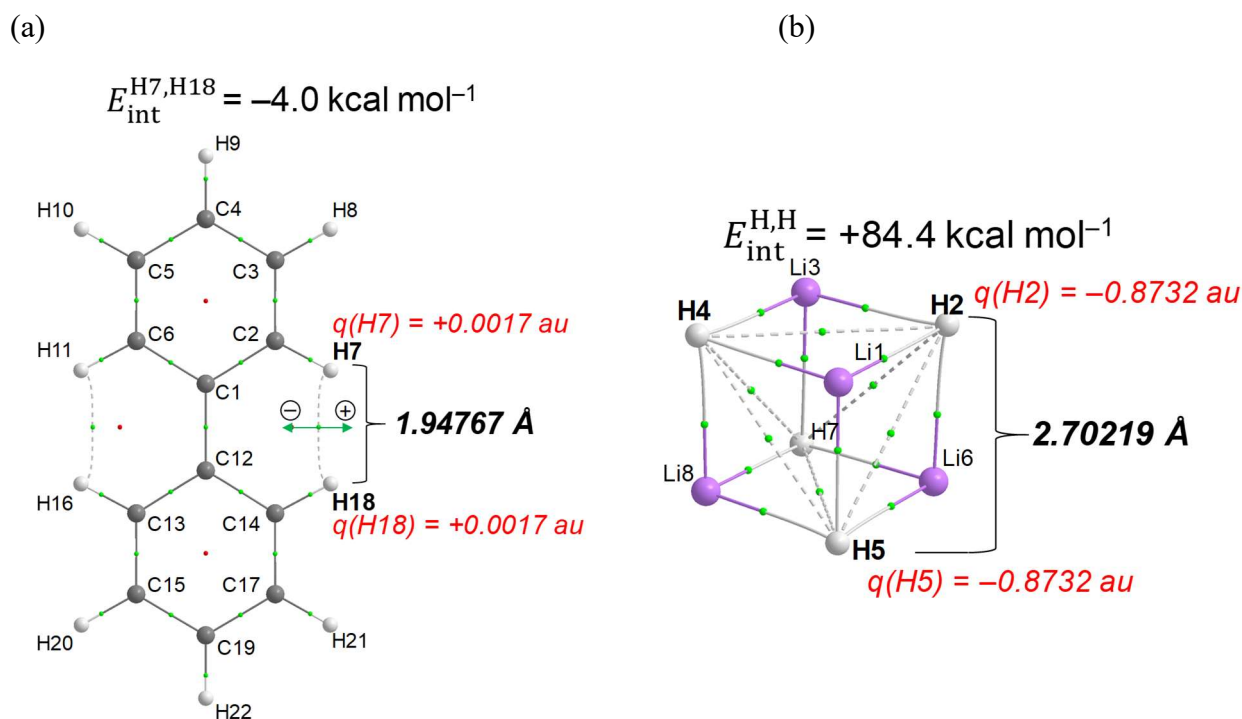


**Figure 1.** Molecular graphs of (a) planar biphenyl and (b) equilibrium structures of cubic Li<sub>4</sub>H<sub>4</sub> calculated at the B3LYP–GD3/6-311++G(2pd,2df) level. The green and red dots represent (3,-1) and (3,+1) critical points, respectively.

Notably, we selected two distinctively different BP-linked homo-polar H,H atom-pairs. In the first instance, the H-atoms in the planar Bph are involved in a weak attractive interaction, have a small positive net atomic charge,  $Q(\text{H})$ , and overlap due to  $d(\text{H,H}) \ll$  the sum of their van der Waals (vdW) radii. In the second case, the H-atoms in  $\text{Li}_4\text{H}_4$  are involved in a very strong repulsive interaction, carry a large negative  $Q(\text{H})$  and are well separated with  $d(\text{H,H}) \gg$  the sum of H-atoms vdW radii. In the latter case and totally unexpectedly, six BPs originating from each H-atom, involving three Li,H and three H,H atom-pairs, are present – Figure 1b.

## 2. METHODS

**2.1. Theoretical Background.** We utilize the recently introduced MO-ED and MO-DI methods,<sup>50</sup> a brief description of our approach is detailed below while a full description of both methods is given in PART 1 of the Supporting Information, SI. Notably, the MO-ED method decomposes the total electron density at a specifically selected coordinate  $\mathbf{r}^*$  into contributions made by each orbital:

$$\rho(\mathbf{r}^*) = \sum_i^{N_{MO}} v_i |\chi_i(\mathbf{r}^*)|^2 \quad (1)$$

where  $\chi_i$  is an MO with occupation  $v_i$ .  $\mathbf{r}^*$  is chosen to be a (3,-1) critical point (CP, or bond critical point) if present, or otherwise the coordinate of a minimum density point (MDP) along an inter-nuclear vector.

The decomposition is then followed along the eigenvector associated with the second eigenvalue of the Hessian matrix which we will refer to as the  $\lambda_2$ -eigenvector. In most cases, the  $\lambda_2$ -eigenvector is synonymous with a cross-section perpendicular to a given inter-nuclear vector. We then consider, for each MO, the partial directional second derivatives computed along the  $\lambda_2$ -eigenvector. From that, each MO can be labelled as *concentrating* ED (negative second derivative), *depleting* ED (positive second derivative) or *non-contributing* to the ED (in the case of an MO node) at the selected  $\mathbf{r}^*$ . Typically, the nature of a selected MO varies at

different CPs/MDPs. MOs' contributions of the same fashion can then be grouped to provide a 'characterized' total density contribution of specific natures at  $\mathbf{r}^*$ :

$$\rho(\mathbf{r}^*) = \rho_{\text{concentrating}}(\mathbf{r}^*) + \rho_{\text{depleting}}(\mathbf{r}^*) + \rho_{\text{non-contributing}}(\mathbf{r}^*) \quad (2)$$

We also make use of recently-developed<sup>51</sup>  $CP(\mathbf{r})$  function to explain the presence of a bond path. This function accounts for the first derivatives computed on the total *concentrating*, *depleting* and *non-contributing* density terms in Eq. 2:

$$CP(\mathbf{r}) = -\text{sign}(\partial\rho_{\text{depleting}}(\mathbf{r})) \cdot [\partial\rho_{\text{concentrating}}(\mathbf{r}) + \partial\rho_{\text{depleting}}(\mathbf{r}) + \partial\rho_{\text{non-contributing}}(\mathbf{r})] \quad (3)$$

Specifically, the  $CP(\mathbf{r})$  is positive in the vicinity of  $\mathbf{r}$  if the slope computed along the  $\lambda_2$ -eigenvector on density provided by the MOs concentrating ED is greater and opposite in sign than the slope obtained for the MOs depleting ED. We have previously found<sup>51</sup> that the  $CP(\mathbf{r})$  will always be positive in the vicinity of a DB. For more details, please refer to Part 1 of the SI.

The MO-DI method, on the other hand, provides a MO-based decomposition of the QTAIM-defined delocalization index (DI). Such a matrix is obtained by first defining an atomic overlap matrix for an atom A with elements

$$S_{ij}^A = \sum_{ij} \int_A \sqrt{v_i} \sqrt{v_j} \chi_i^*(\mathbf{r}) \chi_j(\mathbf{r}) d\mathbf{r} \quad (4)$$

which satisfies  $N(A) = \text{tr}(\mathbf{S}^A)$ , where  $N(A)$  is the total electronic population. A delocalized density matrix for atom-pair A,B can then be defined, with elements

$$D_{ij}^{(A,B)} = 2| -S_{ij}^A S_{ji}^B | \quad (5)$$

where all elements sum up to the QTAIM-defined DI(A,B). The  $\mathbf{D}^{(A,B)}$  matrix provides information regarding the overlap and interference of MOs across two atomic basins. Diagonal elements,  $D_{ii}^{(A,B)}$ , provide each MO's contribution to the total number of electron pairs shared between A and B. This term results from mutual overlap of an MO across two atomic basins.

However, the off-diagonal elements,  $D_{i \neq j}^{(A,B)}$ , provide the extent to which an MO-pair either increases delocalized electron pairs (through constructive interference) or decreases delocalized electron pairs (through deconstructive interference). Therefore, the sum of any row or column of  $\mathbf{D}_{ij}$  gives the net contribution of an MO to the number of electron pairs shared between atoms A and B, after any MO-pair interference effects have been taken into account. An example of such a matrix as well as its interpretation are shown in Part 2 of the SI.

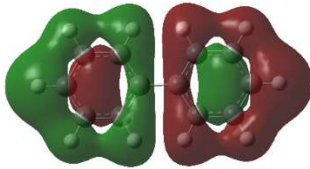
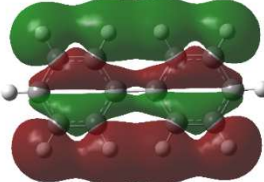
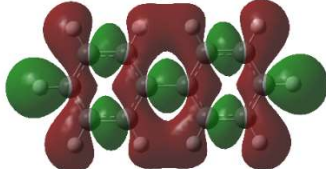
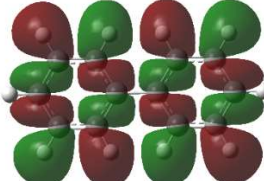
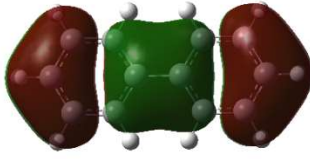
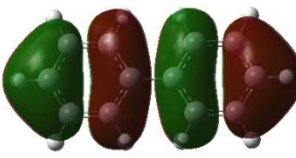
Finally, note that we prefer to use the density bridge (DB) term instead of BP as it perfectly describes the presence of a common topological property of electron density between any pair of atoms in a molecular environment.

**2.2. Computational Details.** All structures were computed in Gaussian 09, Rev. D<sup>52</sup> using B3LYP with Grimme's D3 empirical dispersion<sup>53</sup> with 6-311++G(2df,2pd) in the gas phase; a full set of X,Y,Z coordinates of all molecules discussed in this work is provided in PART 2 in the SI. QTAIM molecular graphs were calculated using AIMAll v. 19.02.13.<sup>54</sup> Molecular orbital density data was obtained using in-house software.

### 3. RESULTS AND DISCUSSION

Both MO-ED and MO-DI methods<sup>50</sup> employ canonical, molecule-wide orbitals without any transformation. Moreover, no partitioning of molecules is required; hence, molecules' structural integrity is fully preserved, an approach not commonly adopted in previous MO-based studies. MOs relevant to this study are shown in Table 1 (a full set of MOs computed for the planar and twisted conformers of Bph are in PART 3 of the SI). Looking at the MO isosurfaces, they are remarkably alike in both Bph conformers. Unfortunately, the shape-similarity does not provide any clue as to why a DB is present (or absent) and hence does not provide any information on whether a MO *concentrates* or *depletes* density anywhere in 3D space occupied by a molecule.

**Table 1.** Selected top-views of MOs in planar Bph. Percentage contributions to ED at relevant BCPs and DI for interactions of interest are also shown.

Orbital	Isosurface	Interaction	% ED	% DI
$\chi_{24}$		H7,H18	0% <i>non-contributing</i>	-6.16 %
		C1,C12	0% <i>non-contributing</i>	-0.41%
		C19,H22	19.9% <i>concentrating</i>	20.17%
$\chi_{29}$		H7,H18	19.1% <i>concentrating</i>	33.13%
		C1,C12	0% <i>non-contributing</i>	0.13%
		C19,H22	8.3% <i>concentrating</i>	-0.01%
$\chi_{36}$		H7,H18	19.1% <i>concentrating</i>	9.25%
		C1,C12	24.3% <i>concentrating</i>	15.45%
		C19,H22	8.3% <i>concentrating</i>	6.62%
$\chi_{37}$		H7,H18	0% <i>non-contributing</i>	-10.10%
		C1,C12	0% <i>non-contributing</i>	-0.61%
		C19,H22	0% <i>non-contributing</i>	0.14%
$\chi_{38}$		H7,H18	0% <i>non-contributing</i>	0.02%
		C1,C12	0% <i>depleting</i>	9.41%
		C19,H22	0% <i>depleting</i>	1.10%
$\chi_{41}$		H7,H18	0% <i>non-contributing</i>	-0.02%
		C1,C12	0% <i>non-contributing</i>	-4.86%
		C19,H22	0% <i>depleting</i>	1.13%

One must realise that just a single set of canonical MOs is always computed for any polyatomic molecule and the molecule-specific electron density distribution is the result of combined individual MO's contributions. However, the ED distribution is not uniform throughout and each molecule has a specific set of covalent bonds and intramolecular, either attractive or repulsive, interactions. From this it follows that a molecule-wide MO cannot have

an overall (non)bonding character. Clearly, each MO's nature, in terms of concentrating, depleting or non-contributing to ED at a specific point  $\mathbf{r}$  in 3D space (such as a critical point on Bader's molecular graphs) can only be established by exploring an inter-nuclear region of an atom-pair of interest.

The second derivative of the ED is associated with electron concentration or depletion in the inter-nuclear region or, for that matter, any point in 3D space occupied by a molecule.<sup>14</sup> We have established that the lowest energy MOs involving C<sub>1s</sub> core electrons in Bph are (i) entirely C-atom-centred and (ii) non-contributing to ED at and in the vicinity of CPs of interest in this work, namely CP/MDP(H7,H18) in planar/twisted Bph and CP(C1,C12) and CP(C19,H22) in planar Bph.

**3.1. MO-based picture of the C1–C12 and C19–H22 covalent bonds in the planar conformer.** We investigate here the carbon-carbon linker (C1–C12) and one of the C–H bonds (C19–H22) as these atoms are not involved in any discernible non-covalent interaction – see Figure 2. A full set of results pertaining to CP(C1,C12) and CP(C19,H22) in the planar conformer is presented in Part 4 of the SI.

Importantly, regardless of the impact made by a local environment, the same and characteristic overall trends are observed for both covalent bonds, namely:

- 1) The directional second partial derivative (from now on called 2<sup>nd</sup> derivative) computed on the *total* ED is negative at both CPs(A,B) seen in Figures 2a,b. Naturally, the 2<sup>nd</sup> derivative is also negative in the vicinity of these CPs showing that ED became highly concentrated in the wider inter-nuclear regions. The trends observed in Figures 2a,b can be seen as a MO-ED signature of an overlap of atomic  $\sigma$ -orbitals that lead to the ED concentration, exactly as one would expect from covalent bonds' classical interpretation.
- 2) Traces of the 2<sup>nd</sup> derivative  $< 0$  shown in Figures 2c,d are signatures of individual MOs that concentrate ED. Typically, only few MOs concentrate ED at a specific CP/MDP and examples



for MOs with %-contributions to the total ED at a CP larger than 10% are shown in Figures 2c,d.

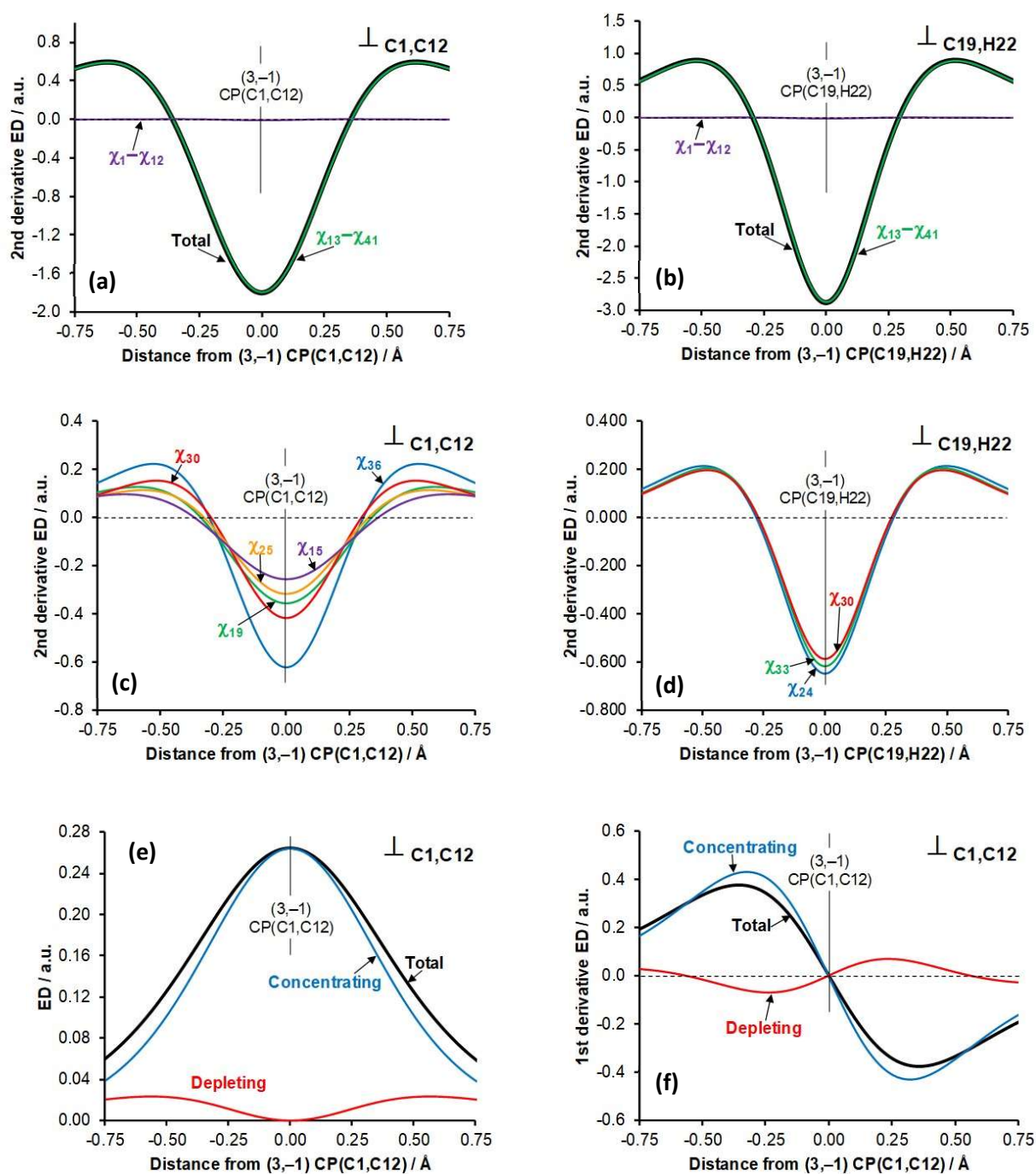


**Figure 2.** Cross-sections along the  $\lambda_2$ -eigenvector in the C1,C12 and C19,H22 inter-nuclear regions. (a) to (d) – MO contributions to directional partial second derivative for C1,C12 or C19,H22, as indicated, and total ED (e) and directional partial first derivative (f) along the  $\lambda_2$ -eigenvector, as selected individual MOs (a and b), grouped according to the contributions from the core ( $\chi_1-\chi_{12}$ , purple line) and valence ( $\chi_{13}-\chi_{41}$ , green line) MOs (c and d) or as the sum of all concentrating (blue) or depleting (red) MOs (e and f).

- 3) The overall combined contribution made by MOs 13-41 is of concentrating nature and the total ED peaks exactly at the relevant CP(A,B) – Figure 2e. There are also MOs that deplete ED in the vicinity of CPs, hence they are classified as such, but they are entirely non-contributing exactly at the CP's coordinates because  $|\chi_i(\text{CP})|^2 = 0.0$ . All these MOs are of  $\pi$  nature in the inter-nuclear region with a node at exactly the relevant CP as shown in Figure 2e.
- 4) The first derivative on the total ED is crossing at the coordinates of CPs(A,B), i.e., at the 0.0 value in Figure 2f.
- 5) The  $CP(\mathbf{r})$  function (developed recently<sup>51</sup> to explain the presence, or otherwise, of a DB) shows that the net slope of all concentrating MOs is greater in magnitude and opposite in sign than the net slope of all depleting MOs at a CP(A,B).

As seen from Figure 2 and Table S6, Figures S3 and S4, Part 4 in the SI, all occupied MOs that contribute to ED at CPs throughout a molecule do so differently in each inter-nuclear region, e.g.,  $\chi_{36}$ , in planar Bph, makes the largest contribution at CP(C1,C12) yet a very small contribution at CP(C19,H22), whereas  $\chi_{24}$  contributes most at CP(C19,H22) but null at CP(C1,C12). Furthermore, the 2<sup>nd</sup>-derivative-defined nature of each MO's contribution (concentrating, depleting and non-contributing) is inter-nuclear region specific – see Table S6, Part 4 of the SI.

To fully understand the role played by each individual MO and quantify its participation in electron delocalization across two atomic basins, one can make a use of the MO-DI protocol (Tables S7-S9, Part 4 of the SI). It quantitatively accounts for positive or constructive (in-phase) and negative or destructive (out-of-phase) interference computed for each unique MO-pair. The net (or total) number of electron pairs delocalized (delocalization index, DI) between C1,C12 and C19,H22 atom-pairs is 1.06 and 0.97, respectively corresponding to a single covalent bond order. The MO-DI method also explains how the covalent bond order comes about, by calculating the overlap of each MO across two atomic basins as well as the interference with all other MOs. Investigation of specific MO-pairs using the MO-DI method

reveals useful insights and strong links to classical MO interpretations. For instance, the core  $1s$   $\chi_1$  and  $\chi_2$  orbitals contribute  $1.0 e^-$ -pairs to  $DI(C1,C12)$  as they completely overlap C1 and C12. However, due to their complete deconstructive interference with each other resulting in  $-1.0 e^-$ -pairs, they do not make a net contribution to  $DI(C1,C12)$  at all. This is an example of a typical bonding-antibonding MO-pair, in full agreement with a classical interpretation of these orbitals. This is a common pattern even among the valence orbitals, such as the  $\chi_{38}$  and  $\chi_{41}$  MO-pair with  $\pi$  character.  $\chi_{38}$  and  $\chi_{41}$  contribute a total of  $0.14 e^-$ -pairs to  $DI(C1,C12)$  through joint overlap over the C1/C12 atomic basins, but  $-0.12 e^-$ -pairs are removed due to deconstructive interference with each other. Analysis of individual MO-pairs might be very tedious. However, analysing the combined contributions of *all* MOs proved to be the most insightful: the net  $DI(C1,C12)$  of 1.06 is a result of 25 overlapping MOs, contributing  $\sum_i D_{ii}^{(C1,C12)} = 2.82 e^-$ -pairs but with a net deconstructive interference of  $\sum_{i \neq j} D_{ij}^{(C1,C12)} = -1.76 e^-$ -pairs. This result can be re-stated using chemical jargon: the C–C bond has a maximum bond-order of  $\sim 3$ , which is reduced to  $\sim 1$  due to the presence of bonding-antibonding MO-pairs.

We also note here a strong relationship between our MO-ED and MO-DI results: all of the MOs that concentrate density to an inter-nuclear region also i) strongly overlap both atomic basins, and ii) interfere constructively with each other. This important observation shows that all MOs that concentrate density in an inter-nuclear region are of the same general nature (*i.e.*  $\sigma$ -symmetries) and contribute to the covalency of an interaction.

**3.2. MOs-based interpretation of absence and presence of a DB between H-atoms of a bay in Bph conformers.** All the data and observations detailed above for classical covalent bonds paint a very strong picture of both the nature of MOs involved in the topological definition of a DB, as well as the nature and mechanism of electron delocalization across an interaction. This picture is in a full agreement with a general notion of covalent bonds

formation and their energy-minimising contribution to molecular energy. Hence, we decided to follow exactly the same protocol in investigating inter-nuclear regions between covalently non-bonded H7,H18 atom-pair in both Bph conformers – a full set of data is placed in Part 5 of the SI.

Looking at the MO isosurfaces, all contributing MOs are of a  $\sigma$ -fashion relative to the H $\cdots$ H interaction in both conformers. Examples of cross-sections of MOs that concentrate ED, as identified by the 2<sup>nd</sup> derivative, are shown in Figures 3a,b. The shapes of traces are rather complex (due to congested molecular environment) and the number of concentrating and depleting MOs differs for both conformers. The trends obtained for the total ED revealed (Figures 3c,d) that there is no qualitative difference, as there is a region along the  $\lambda_2$ -eigenvector (including coordinates of CP(H,H) and MDP(H,H)) where the 2<sup>nd</sup>-derivative  $< 0$ . This shows that the overall and dominant effect is ED concentration in the inter-nuclear region that resulted in  $\rho_{CP} = 0.01427$  a.u. (planar) and  $\rho_{MDP} = 0.00529$  a.u. (twisted). Moreover, largely the same orbitals ( $\chi_{23}$ ,  $\chi_{25}$ ,  $\chi_{29}$ ,  $\chi_{35}$  and  $\chi_{36}$ ) concentrate ED between H-atoms to a total of 72.9% and 61.6% in planar and twisted conformers, respectively.

The only significant difference is in the degree and the slope of MOs' contribution to each inter-nuclear region. We found that the overall degree of ED concentration, relative to depletion, is greater in planar (94.5%) than in twisted (71.3%) at respective points (CP and MDP). Individual MOs' contributions produced specific traces in the total ED (Figures 3c,d) that explain the difference in 1<sup>st</sup> derivatives (Figures 3e,f) and hence the presence of a DB(H7,H18) only in the planar Bph. Only in the planar Bph we see the trend (thick solid black line in Figure 3e) computed for the 1<sup>st</sup> derivative on the total ED crossing zero at the exact coordinates of CP(H,H) and the ring critical point (RCP). These critical points are classical topological features when atoms linked by a DB(A,B) form a ring on a molecular graph. The appearance/absence of these two critical points in Figures 3ef is synonymous with the presence/absence of a density bridge, here DB(H7,H18) in the planar Bph.

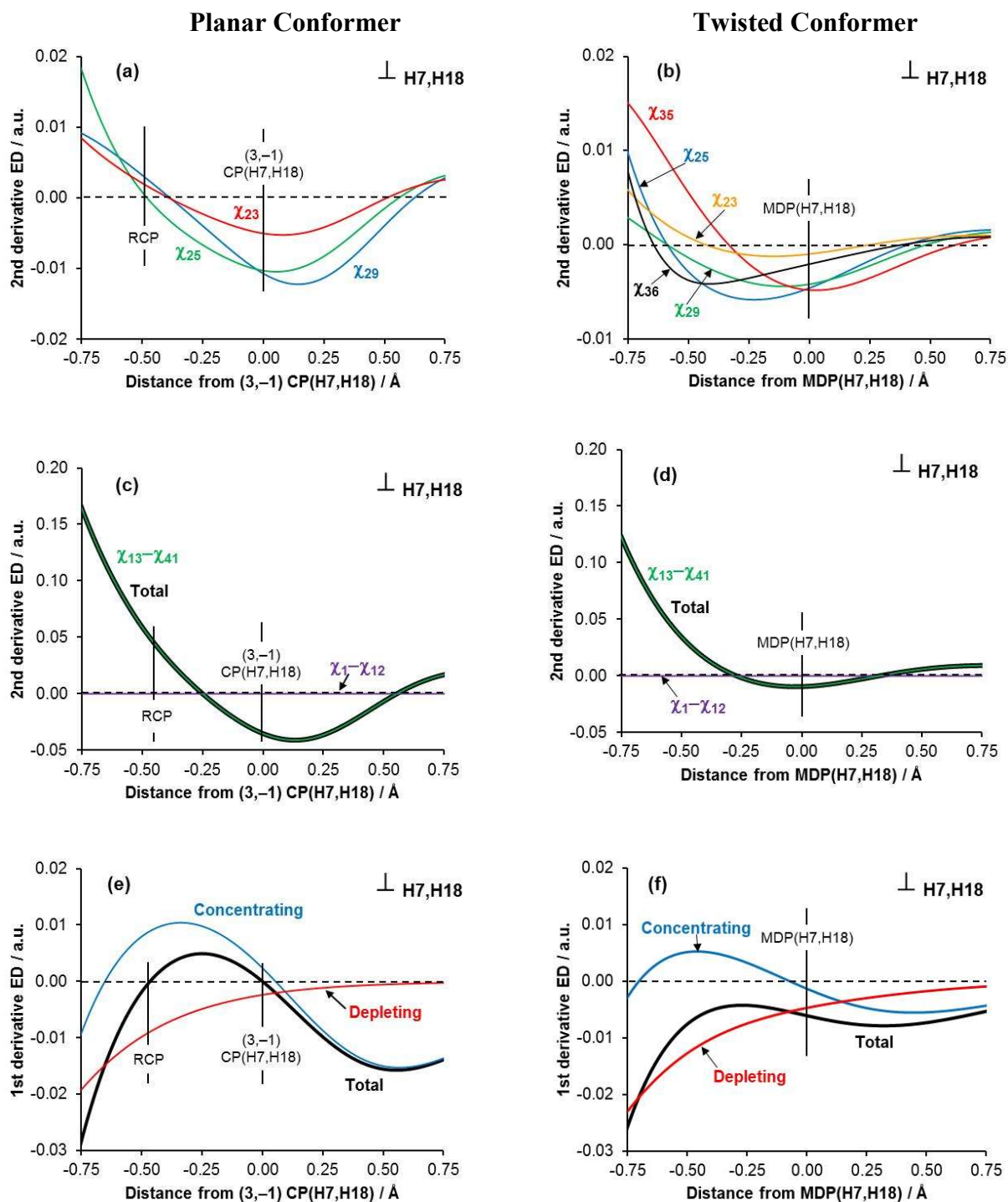


**Figure 3** Decomposition of the directional partial second (a to d) and first (e and f) derivatives along the  $\lambda_2$ -eigenvector in the H7,H18 inter-nuclear region in planar (left) and twisted (right) biphenyl, on selected individual MOs (a and b), grouped according to the contributions from the core ( $\chi_1$ - $\chi_{12}$ , purple line) and valence ( $\chi_{13}$ - $\chi_{41}$ , green line) MOs (c and d) or, for the first derivative, on the sum of all concentrating (blue) or depleting (red) MOs (e and f).

Decomposition of the trace of the total ED (Figures 3e,f) into the sums of concentrating and depleting MOs shows that the rate of change of concentrating MOs is greater than the rate of change of depleting MOs in planar Bph, while the opposite is true for twisted Bph. This single

observation – as confirmed by the  $CP(\mathbf{r})$  function<sup>51</sup> and trends in 1<sup>st</sup> derivatives shown in Figures S5 and S6, Part 5 in the SI – is the only reason for the presence/absence of DB(H7,H18) in planar/twisted Bph.

To gain additional insight on the nature of the H...H interactions in terms of MOs, we used the MO-DI method – see Tables S11 and S12, Part 5 in the SI. They show a decomposition of the QTAIM-defined DI(H7,H18) of 0.031 and 0.011  $e^-$ -pairs in the planar and twisted Bph, respectively, into contributions made by each MO. The MO-DI method takes into account the spatial overlap of an MO across both atomic basins (diagonal values,  $\sum_i D_{ii}^{(H7,H18)}$ ) as well as the constructive or destructive interference of an MO with all remaining MOs (off-diagonal values,  $\sum_{i \neq j} D_{ij}^{(H7,H18)}$ ).

As an example, let us consider  $\chi_{29}$  in planar Bph – the MO that shows in-phase  $\sigma$ -symmetry for most H atoms and out-of-phase  $\sigma^*$ -symmetry for C–H bonds, Table 1. In case of the planar conformer,  $\chi_{29}$  contributes net 0.010  $e^-$ -pairs, *i.e.*, 33% of the DI(H7,H18). This is a result of spatial overlap (0.012  $e^-$ -pairs) and overall interference with other MOs (it amounts to  $-0.002$   $e^-$ -pairs). Most significant constructive interference involves  $\chi_{25}$  (in-phase  $\sigma$ -symmetry for H7,H18) which contributes an additional 0.009  $e^-$ -pairs whereas most significant deconstructive interference involves  $\chi_{37}$  (out-of-phase  $\sigma^*$ -symmetry for H7,H18) which reduces the total DI by  $-0.009$   $e^-$  pairs.

However, the most accurate picture of electron delocalization for the H7...H18 interactions can only be obtained by taking into account the overlap and interferences with all MOs. We note that the same general trend as what was observed for the C1–C12 bond, although to a much lesser degree, holds for the H7...H18 interaction in planar biphenyl. In total, MOs overlapping both H7 and H18 contribute 0.064 delocalized  $e^-$ -pairs, but this gets reduced by  $-0.033$   $e^-$ -pairs as a result of destructive interferences. Very much the same holds true for the H7...H18 interaction in twisted biphenyl. Whereas spatially overlapping MOs contribute to

DI(H7,H18) more or less the same, 0.060  $e^-$ -pairs, the reduction of DI due to net destructive interferences ( $-0.049 e^-$ -pairs) is considerably greater than in the planar biphenyl. This clearly demonstrates that the in-phase MOs' overlap over the H...H interaction is relatively stronger than out-of-phase overlap in planar than twisted biphenyl. In chemical jargon terms, bonding-antibonding MO-pairs reduce the bond order less in planar than twisted biphenyl. Possibly the most important observation, however, is the same nature of MO-overlap as what was observed for the C1–C12 linker in planar Bph: all MOs that concentrate ED at the BCP/MDP(H7,H18) also i) interfere constructively with each other and ii) contribute to the DI in a net-positive fashion.

Taking all of the above results from the MO-ED and MO-DI decompositions into the account, it is abundantly clear that the interaction between H7 and H18 in planar or twisted biphenyl share two critical features. These features, which are also observed for covalent bonds, are: 1) a net concentration of ED in the interatomic region arising from multiple MOs of strictly  $\sigma$ -character and 2) a net delocalization of electron-pairs arising from MO-overlap. Furthermore, our results clearly demonstrate that (i) selecting just few MOs, even with dominant contributions, cannot sufficiently describe the H...H interactions of interest and (ii) it is only through the consideration of all occupied MOs that the topology of the total ED can be recovered and interpreted meaningfully. The only discernible difference between the H...H interactions in planar or twisted biphenyl is the presence of a density bridge. It arises purely from different rates of change of net concentrating relative to depleting MOs' contributions to the total ED, a fact that does not change the underlying nature of the interaction.

**3.3. MO-based nature of the hydride H,H DBs in cubic Li<sub>4</sub>H<sub>4</sub>.** Cubic Li<sub>4</sub>H<sub>4</sub> is an interesting molecule as its molecular graph reveals six density bridges originating from each H-atom. Even more surprising is the presence of three DBs(HH) linking each H-atom with the remaining ones despite (i)  $d(\text{HH}) \gg$  the sum of the vdW radii by 0.30 Å and (ii) each H-atom

being involved in three large repulsive interactions with neighbouring H-atoms. The computed  $E_{\text{int}}^{\text{H,H}} = +84.4 \text{ kcal mol}^{-1}$  is dominated by the classical electrostatic Coulomb energy term of  $V_{\text{cl}}^{\text{H,H}} = +92.6 \text{ kcal mol}^{-1}$ .

There are 2 groups of 4 doubly-occupied MOs:  $\chi_1$ – $\chi_4$  are formed from  $1s_{\text{Li}}$  whereas  $\chi_5$ – $\chi_8$  from  $1s_{\text{H}}$  orbitals – Figure 4. Each group of MOs consists of a single, symmetrical and in-phase MO as well as three degenerate orbitals of different symmetry combinations. Together, this set of 8 MOs describes 24 interactions, 12 Li–H, 6 Li...Li and 6 H...H, and interestingly, density bridges are present for all Li–H and H...H but Li...Li interactions.

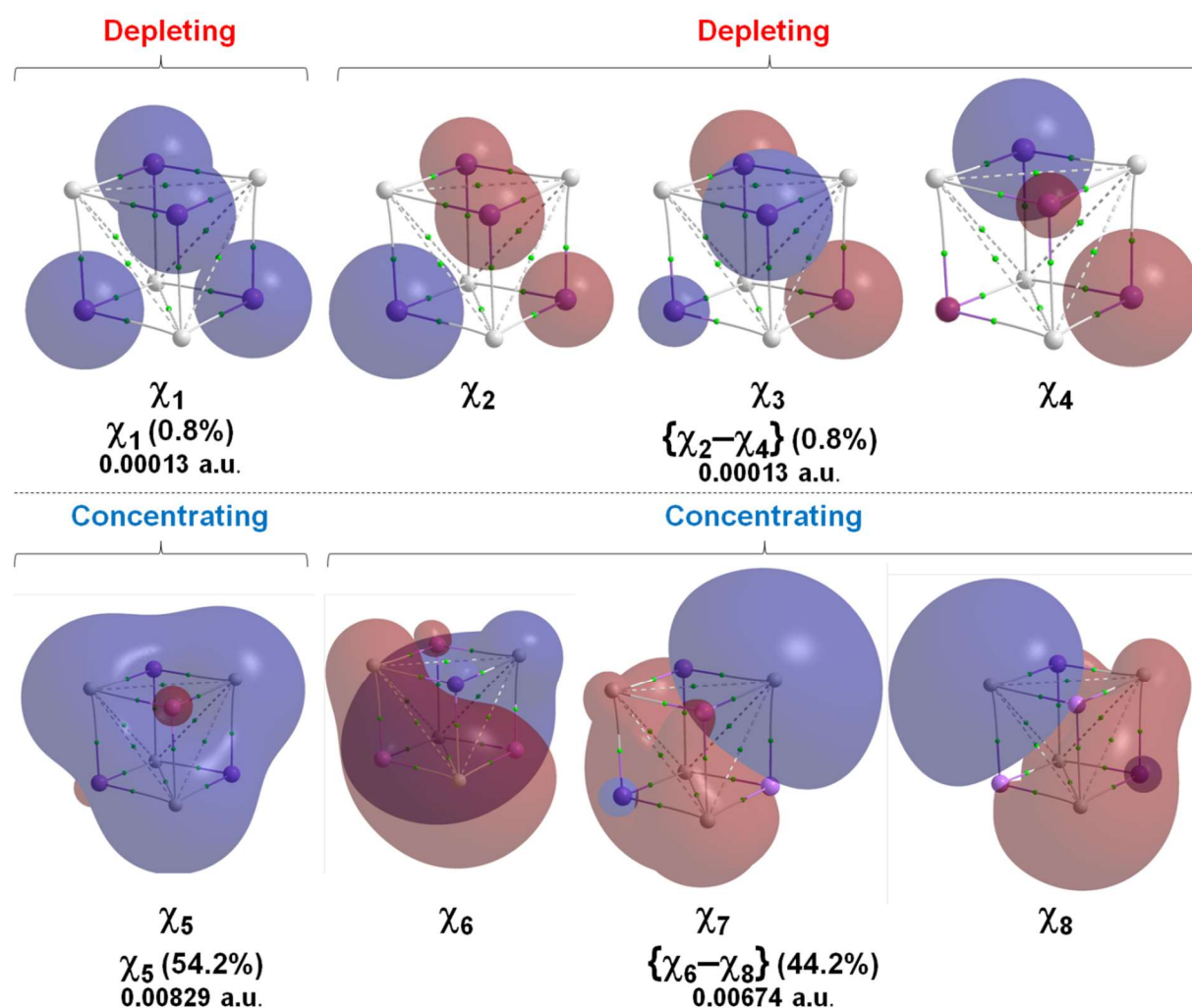


**Figure 4.** Shapes of the eight MOs in cubic  $\text{Li}_4\text{H}_4$  (isovalue = 0.02 a.u.). The nature of each MOs contribution to a single H...H interaction, as defined by the sign of the 2<sup>nd</sup>-derivative, is shown.



We are particularly interested in explaining the presence of the DBs between hydride atoms and due to perfect symmetry of cubic  $\text{Li}_4\text{H}_4$ , we will discuss the H2,H5 atom-pair as an example – a full set of relevant data is included in Part 6 in the SI. The 2<sup>nd</sup> derivative trends seen in Figure 5a reveal that concentrating in nature contributions to ED of 0.01530 a.u. at the CP(H2,H5) are made only by  $\chi_5$ – $\chi_8$  MOs. This is because the 2<sup>nd</sup> derivative  $< 0$  is observed at and in the vicinity of the CP(H2,H5). These orbitals contribute 98.3% to ED at this CP with 54.2% coming from  $\chi_5$  (Figure 5b). The remaining 1.7% of ED at the CP(H2,H5) comes from four MOs ( $\chi_1$ – $\chi_4$ ) in a depleting fashion (Figure 5c) with  $\chi_1$  adding 0.8%.

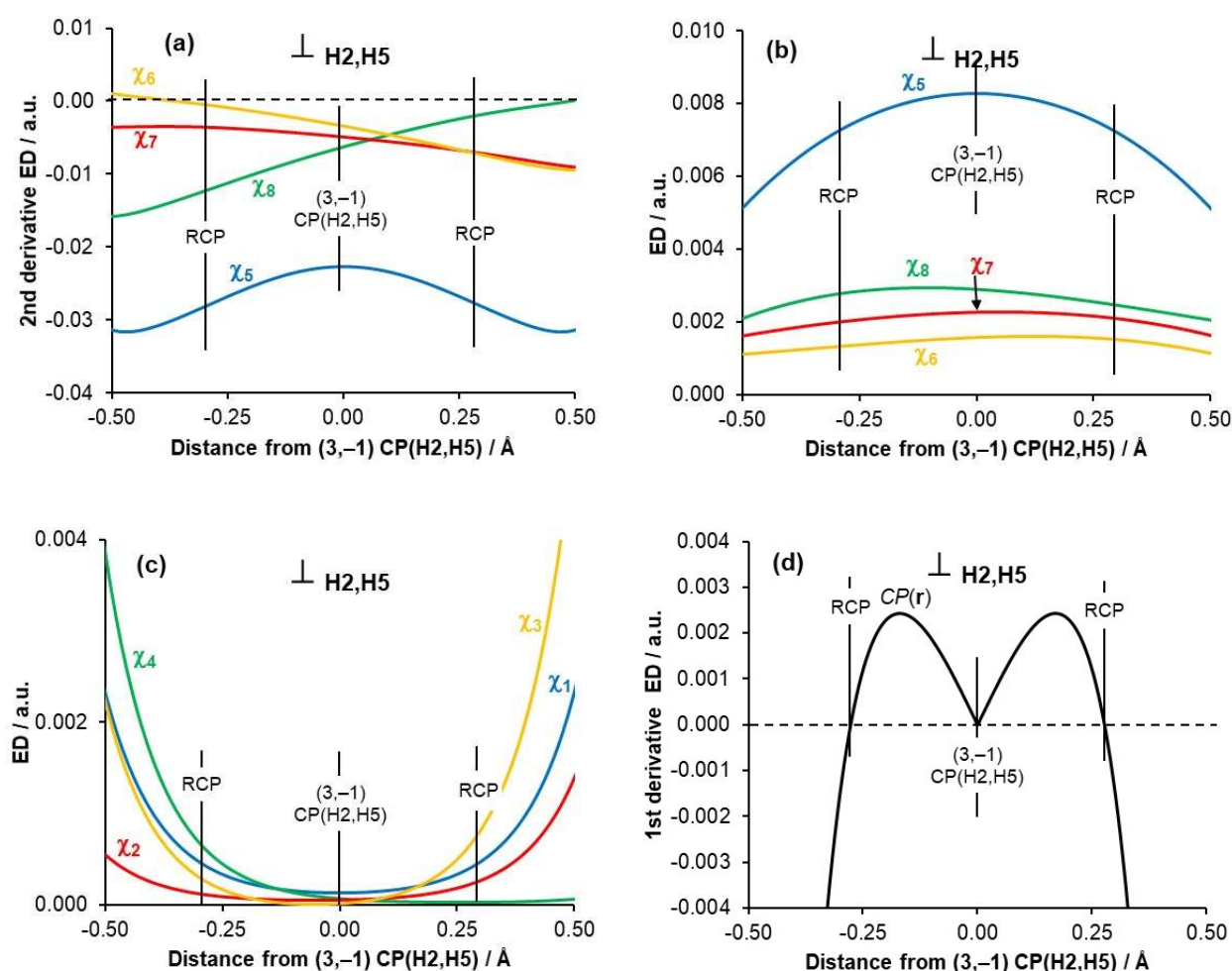


**Figure 5.** The partial directional 2<sup>nd</sup>-derivative (a), ED contributions made by higher-energy MOs ( $\chi_5$ – $\chi_8$ , b) and lower-energy MOs ( $\chi_1$ – $\chi_4$ , c) and the  $CP(\mathbf{r})$  function (d) as cross-sections along the  $\lambda_2$ -eigenvector for atom-pair H2,H5 in  $\text{Li}_4\text{H}_4$ .

The three degenerate orbitals of different symmetry, ( $\chi_2$ - $\chi_4$ ) and ( $\chi_6$ - $\chi_8$ ), make combined identical contributions to ED at all three CP(H,H), namely 0.0013 and 0.0674 au, respectively. However, individual MO's contributions vary dramatically, *e.g.*, for  $\chi_6$  we obtained 0.0, 10.4 and 33.8 %-contributions to CP(H2,H4), CP(H2,H5) and CP(H4,H5), respectively – see Table S14 in Part 6 of the SI. As for the H...H interaction in planar Bph, the DBs between H-atoms in Li<sub>4</sub>H<sub>4</sub> are present as a result of the greater slope of the total concentrating than depleting ED contributions made by MOs (Figure 5d).

The MO-DI results obtained for the representative H2...H5 interaction (Table S15, Part 6 of the SI) show that  $\chi_1$  localised on all four Li nuclei contributes negligibly to DI(H,H), through both overlap and constructive interference with other MOs. The DI(H2,H5) arises predominantly from the overlap of  $\chi_5$  (contributing 0.21  $e^-$ -pairs) and the combined overlap of  $\chi_6$ - $\chi_8$  (contributing a sum of 0.15  $e^-$ -pairs) to a total of 0.36  $e^-$ -pairs. However,  $\chi_5$  also interferes destructively with  $\chi_6$ - $\chi_8$  and this reduces the total DI(H,H) by -0.26  $e^-$ -pairs. Hence, a small but not insignificant net total DI(H2,H5) = +0.09  $e^-$ -pairs was obtained. This observation confirms the classical closed-shell nature of the H...H interactions as the  $\chi_5$  and  $\chi_6$ - $\chi_8$  MOs form a seemingly bonding-antibonding pair, although in slight favour of net covalent character.

## Conclusions

This work unambiguously shows that physical processes leading to appearance of density bridges (DBs) are exactly the same regardless of the strength and nature of interaction atoms are involved in. We report the MO-based interpretation of:

1. Classical C–C and C–H covalent bonds in the Bph. They represent very strong and overall attractive interactions due to dominant contribution coming from the exchange

correlation term (XC-term). In both cases, an electron-pair sharing (hence electron density concentration) in the inter-nuclear region takes place.

2. A steric CH...HC contact in the non-equilibrium planar conformer of Bph. It is characterised by a weak and slightly attractive, due to dominance of the XC-term, interaction between homo-polar H-atoms.
3. A very large repulsive, due to dominance of electrostatic term, H...H interaction in the *equilibrium structure* of cubic Li<sub>4</sub>H<sub>4</sub>. Remarkably, each H-atom is involved in three such repulsive, over +80 kcal mol<sup>-1</sup>, interactions.

We have fully explained the appearance of DBs using the MO-ED and MO-DI protocols reported by us recently.

We used the directional second partial derivative (2<sup>nd</sup>-derivative) computed on the total electron density (ED) along the  $\lambda_2$ -eigenvector crossing a critical, or minimum density, point (CP or MDP) on a Bader's molecular graph. The negative value of the 2<sup>nd</sup>-derivative was found for all interactions studied and it indicates a net concentration of electron density at and in the vicinity of CPs and MDP studied. In each case investigated, there are sets of MOs that (i) contribute either in concentrating or depleting fashion to the total ED or (ii) make no contribution at exactly the CP's coordinates. All MOs that concentrate ED in an inter-nuclear region also overlap both atomic basins and interfere constructively (in-phase) with other ED-concentrating MOs. Hence, they contribute in a positive fashion to the number of delocalized electron-pairs. Therefore, all MOs that contribute to the presence of a DB (through a concentration of ED) also contribute to the degree of covalency that is conveniently measured by a delocalisation index, DI(A,B).

Notably, the 2<sup>nd</sup>-derivative  $< 0$  is a necessary (although not sufficient) condition for a DB to be present. For a DB to be present the rate of change of concentrating ED must be greater and opposite in sign than the rate of change of depleting ED along the  $\lambda_2$ -eigenvector. Therefore,

the absence of a DB does not indicate the absence of concentrating MOs as it has been demonstrated for the H7,H18 atom-pair in the equilibrium (twisted) Bph.

All the above observations and conclusions are equally applicable to all and so diverse atom-pairs studied in this work. This leads us to the final conclusion regarding the MO's nature of DBs: *a DB indicates the presence of MOs that concentrate ED in an interatomic region and increase the degree of covalency of the relevant interaction, but the absence of a DB does not indicate the absence of such MOs.*

What is then the significance of a DB? Is there a universal attribute that could be used to describe the role played by a DB in a molecular system? It is well-known fact that the formation of covalent bonds (synonymous with ED sharing) decreases the energy of a molecular system, generally through orbital-expansion and regardless of a kinetic or potential energy driving force.<sup>55</sup> We have shown that this key property applies to MOs that contribute constructively to the formation of a DB. From the fact that processes leading to the appearance of any DB are the same, regardless of which atom-pair becomes linked by a DB, it follows that the energy-lowering effect must be applicable to all of them. In other words, formation of a specific set of DBs (in most cases they represent classical covalent bonds) exemplifies the manner in which a molecular system is distributing its density such that at a particular 3D placement of nuclei the electronic energy of the system is at its minimum.

One can also consider another scenario. The optimum geometry of a molecule is obtained from energy-optimisation protocols implemented in all major dedicated software packages. The resultant density distribution, incorporating density bridges as observed on Bader's molecular graphs, can be fully recovered from combined individual MO's contributions. Hence, the final set of MOs in an equilibrium structure represents lowest energy density distribution.

A DB has also been interpreted<sup>33</sup> as a '*privileged exchange channel*', which – according to some<sup>56</sup> – shows that a DB is present between two atoms as a result of the greatest exchange-

correlation stabilization out of multiple, competing ‘*exchange channels*’. Whilst this concept has been challenged recently,<sup>57</sup> some of us have previously shown<sup>58</sup> that the significant multi-centric character of many DBs makes the concept of ‘*privilege*’ quite hard to interpret and even more so to quantify. Upon the request of a reviewer, we can restate the concept of exchange channels in terms of MOs: an exchange channel can be seen as a product of the set of MOs that both concentrate ED and contribute to interatomic electron delocalization in a specific inter-nuclear region. We have shown that such a set of MOs will always be present if a DB is present. It is then tempting to also link the concept of ‘*privilege*’ with the relative slopes as per the  $CP(\mathbf{r})$  function (see Eq. 3), but to do so will require careful consideration of a significant number of different and often highly controversial systems. We will be exploring these links in a future publication.

From all these final remarks it follows that a common attribute of a DB is its energy-minimising contribution to a molecular system. Also, by analogy to chemists’ understanding of covalent bonds, it is also clear that the presence of a DB is synonymous with a physical process of chemical bonding between two atoms that always stabilises a molecule. Bonding is a physical process that might, but does not have to, lead to the formation of a chemical bond as commonly understood by a chemist at large. Finally, bonding as a universal physical process can take place without being pin-pointed by the appearance of a DB. The H7,H18 atom-pair in a twisted conformer of Bph is an excellent example of such phenomenon. This work revealed that the only discernible difference between the H...H interactions in planar or twisted biphenyl arises purely from different rates of change of net concentrating relative to depleting MOs’ contributions to the total ED. The presence of a density bridge in the case of the planar conformer of Bph, does not change the fact that MOs delocalizing  $e^-$ -pairs and concentrating ED do dominate in both conformers.

It is our conviction that this work levels the ground for harmonious, cooperative and complementary research conducted by orbital- and electron density-based camps when, at least,

describing and characterising any possible interaction and chemical bond in all molecular structures is of interest.

## Notes

The authors declare no competing financial interest.

## ASSOCIATED CONTENT

### Supporting Information

The Supporting Information is available free of charge at

Cartesian coordinates for all optimized molecules, **Part 1**. Theoretical background for the MO-ED and MO-DI methods, **Part 2**. Isosurfaces for all canonical MOs in planar and twisted Bph, **Part 3**. Complete characterization and decomposition of the ED at CP(C1,C12) and CP(C19,H22), tabulated and visualized; truncated as well as summarized tables of MO overlap and interferences for C1,C12 and C19,H22 atom-pairs, **Part 4**. Complete characterization and decomposition of the ED at CP(H7,H18) and MDP(H7,H18) in planar and twisted Bph, respectively, tabulated and visualized; truncated as well as summarized tables of MO overlap and interferences for H7,H18 atom-pair in planar and twisted Bph, **Part 5**. Complete characterization and decomposition of the ED at CP(H2,H4), CP(H2,H5) and CP(H4,H5) in Li<sub>4</sub>H<sub>4</sub>, tabulated and visualized; full table of MO overlap and interference for atom-pair H2,H5 in Li<sub>4</sub>H<sub>4</sub>, **Part 6**.

## ACKNOWLEDGMENTS

The authors gratefully acknowledge the Centre for High Performance Computing (CHPC), South Africa, for providing computational resources to this research project and National Research Foundation of South Africa, Grant Number 105855, for financial support.

## REFERENCES

- (1) *The Chemical Bond: Fundamental Aspects of Chemical Bonding*; Frenking, G., Shaik, S., Eds.; Wiley-VCH Verlag GmbH, & Co, KGaA, Weinheim, Germany, 2014.
- (2) *The Chemical Bond: Chemical Bonding Across the Periodic Table*; Frenking, G., Shaik, S., Eds.; Wiley-VCH Verlag GmbH & Co, KGaA, Weinheim, Germany, 2014.
- (3) Bickelhaupt, F. M.; Baerends, E. J. In *Reviews in Computational Chemistry*; Lipkowitz, K. B., Boyd, D. B. Eds.; VCH: New York, 2000; Vol. 15, Chapter 1.
- (4) Ziegler, T.; Rauk, A. Carbon monoxide, carbon monosulfide, molecular nitrogen, phosphorus trifluoride, and methyl isocyanide as sigma donors and pi acceptors. A theoretical study by the Hartree-Fock-Slater transition-state method. *Inorg. Chem.* **1979**, *18*, 1755–1759.
- (5) Wu, W.; Song, L.; Cao, Z.; Zhang, Q.; Shaik, S. Valence bond configuration interaction: a practical ab initio valence bond method that incorporates dynamic correlation, *J. Phys. Chem. A*, **2002**, *106*, 2721–2726.
- (6) Song, L.; Wu, W.; Zhang, Q.; Shaik, S. A practical valence bond method: a configuration interaction method approach with perturbation theoretic facility. *J. Comput. Chem.* **2004**, *25*, 472–478.
- (7) Weinhold, F.; Landis, C. R. *Valency and bonding. A natural bond orbital donor–acceptor perspective*; Cambridge University Press: Cambridge, U.K., 2005.
- (8) Weinhold, F. Rebuttal to the Bickelhaupt–Baerends case for steric repulsion causing the staggered conformation of ethane. *Angew. Chem. Int. Ed.* **2003**, *42*, 4188–4194.
- (9) Weinhold, F.; von Ragué Schleyer, P.; McKee, W. C. Bay-type H···H “bonding” in *cis*-2-butene and related species: QTAIM versus NBO description. *J. Comput. Chem.* **2014**, *35*, 1499–1508.
- (10) Mitoraj, M. P.; Michalak, A.; Ziegler, T. On the nature of the agostic bond between metal centers and  $\beta$ -hydrogen atoms in alkyl complexes. An analysis based on the extended transition state method and the natural orbitals for chemical valence scheme (ETS-NOCV). *Organometallics* **2009**, *28*, 3727–3733.
- (11) Mitoraj, M. P.; Michalak, A.  $\sigma$ -donor and  $\pi$ -acceptor properties of phosphorus ligands: An insight from the natural orbitals for chemical valence. *Inorg. Chem.* **2010**, *49*, 578–582.
- (12) Mitoraj, M. P.; Parafiniuk, M.; Srebro, M.; Handzlik, M.; Buczek, A. Michalak, A. Applications of the ETS-NOCV method in descriptions of chemical reactions. *J. Mol. Model.* **2011**, *17*, 2337–2352.

- (13) Cukrowski, I.; Sagan, F.; Mitoraj, M. P. On the stability of *cis*- and *trans*-2-butene isomers. An insight based on the FAMSEC, IQA, and ETS-NOCV schemes. *J. Comput. Chem.* **2016**, *37*, 2783–2798.
- (14) Bader, R. F. W. *Atoms in Molecules. A Quantum Theory*: Oxford University Press: Oxford, Great Britain, 1990.
- (15) Gillespie, R. J.; Popelier, P. L. A. *Chemical bonding and molecular Geometry. From Lewis to electron density*; Oxford University Press, Oxford, U.K., 2001.
- (16) Bader, R. F. W.; Fang, D.-C. Properties of atoms in molecules: caged atoms and the Ehrenfest force. *J. Chem. Theory Comput.* **2005**, *1*, 403–414.
- (17) Blanco, M. A.; Pendás, A. M.; Francisco, E. Interacting quantum atoms: a correlated energy decomposition scheme based on the quantum theory of atoms in molecules. *J. Chem. Theory Comput.* **2005**, *1*, 1096–1109.
- (18) Tiana, D.; Francisco, E.; Blanco, M. A.; Macchi, P.; Sironia, A.; Pendás, A. M. Restoring orbital thinking from real space descriptions: bonding in classical and non-classical transition metal carbonyls. *Phys. Chem. Chem. Phys.* **2011**, *13*, 5068–5077.
- (19) Pendás, A. M.; Blanco, M. A.; Francisco, E. Steric repulsions, rotation barriers, and stereoelectronic effects: a real space perspective. *J. Comput. Chem.* **2009**, *30*, 98–109.
- (20) Geldof, D.; Krishtal, A.; Blockhuys, F.; Van Alsenoy, C. An extension of the Hirshfeld method to open shell systems using fractional occupations. *J. Chem. Theory Comput.* **2011**, *7*, 1328–1335.
- (21) Geldof, D.; Krishtal, A.; Blockhuys, F.; Van Alsenoy, C. Quantum chemical study of self-doping PPV oligomers: spin distribution of the radical forms. *Theor. Chem. Acc.* **2012**, *131*, 1243.
- (22) Cukrowski, I. IQA-embedded fragment attributed molecular system energy change in exploring intramolecular interactions. *Comput. Theor. Chem.* **2015**, *1066*, 62–75.
- (23) Cukrowski, I.; van Niekerk, D. M. E.; de Lange, J. H. Exploring fundamental differences between red- and blue-shifted intramolecular hydrogen bonds using FAMSEC, FALDI, IQA and QTAIM. *Struct. Chem.* **2017**, *28*, 1429–1444.
- (24) Cukrowski, I. Reliability of HF/IQA, B3LYP/IQA, and MP2/IQA data in interpreting the nature and strength of interactions. *Phys. Chem. Chem. Phys.* **2019**, *21*, 10244–10260.
- (25) Matta, C. F.; Hernández-Trujillo, J.; Tang, T-H.; Bader, R. F. W. Hydrogen–hydrogen bonding: a stabilizing interaction in molecules and crystals. *Chem. Eur. J.* **2003**, *9*, 1940–1951.
- (26) Echeverría, J.; Aullón, G.; Danovich, D.; Shaik, S.; Alvarez, S. Dihydrogen contacts in alkanes are subtle but not faint. *Nature Chem.* **2011**, *3*, 323–330.



- (27) Cioslowski, J.; Mixon, S. T. Universality among topological properties of electron density associated with the hydrogen–hydrogen nonbonding interactions. *Can. J. Chem.*, **1992**, *70*, 443–449.
- (28) Poater, J.; Solà, M.; Bickelhaupt, F. M. Hydrogen–hydrogen bonding in planar biphenyl, predicted by atoms-in-molecules theory, does not exist. *Chem. Eur. J.* **2006**, *12*, 2889–2895.
- (29) Bader, R. F. W. Pauli repulsions exist only in the eye of the beholder. *Chem. Eur. J.* **2006**, *12*, 2896–2901.
- (30) Poater, J.; Solà, M.; Bickelhaupt, F. M. A model of the chemical bond must be rooted in quantum mechanics, provide insight, and possess predictive power. *Chem. Eur. J.* **2006**, *12*, 2902–2905.
- (31) Pacios, L. F.; Gómez, L. Conformational changes of the electrostatic potential of biphenyl: A theoretical study. *Chem. Phys. Lett.* **2006**, *432*, 414–420.
- (32) Hernández-Trujillo, J.; Matta, C. F. Hydrogen–hydrogen bonding in biphenyl revisited. *Struct. Chem.* **2007**, *18*, 849–857.
- (33) Pendás, A. M.; Francisco, E.; Blanco, M. A.; Gatti, C. Bond paths as privileged exchange channels. *Chem. Eur. J.* **2007**, *13*, 9362–9371.
- (34) Eskandari, K.; Van Alsenoy, C. Hydrogen–hydrogen interaction in planar biphenyl: A theoretical study based on the interacting quantum atoms and Hirschfeld atomic energy partitioning methods. *J. Comp. Chem.* **2014**, *35*, 1883–1889.
- (35) Jenkins, S.; Maza, J. R.; Xu, T.; Jiajun, D.; Kirk, S. R. Biphenyl: A stress tensor and vector-based perspective explored within the quantum theory of atoms in molecules. *Int. J. Quant. Chem.* **2015**, *115*, 1678–1690.
- (36) Jiajun, D.; Xu, Y.; Xu, T.; Momen, R.; Kirk, S. R.; Jenkins, S. The substituent effects on the biphenyl H···H bonding interactions subjected to torsion. *Chem. Phys. Lett.* **2016**, *651*, 251–256.
- (37) Li, J.; Huang, W.; Xu, T.; Kirk, S. R.; Jenkins, S. A vector-based representation of the chemical bond for the substituted torsion of biphenyl. *Chem. Phys. Lett.* **2018**, *702*, 32–37.
- (38) Jara-Cortés, J.; Hernández-Trujillo, J. Energetic analysis of conjugated hydrocarbons using the interacting quantum atoms method. *J. Comp. Chem.* **2018**, *39*, 1103–1111.
- (39) Popelier, P. L. A. Maxwell, P. I.; Thacker, J. C. R.; Alkorta, I. A relative energy gradient (REG) study of the planar and perpendicular torsional energy barriers in biphenyl. *Theoret. Chem. Acc.* **2019**, *138*, 12.

- (40) Hancock, R. D.; Nikolayenko, I. V. Do nonbonded H<sup>-</sup>-H interactions in phenanthrene stabilize it relative to anthracene? A possible resolution to this question and its implications for ligands such as 2,2'-bipyridyl. *J. Phys. Chem. A* **2012**, *116*, 8572–8583.
- (41) Bastiansen, O.; Samdal, S. Structure and barrier of internal rotation of biphenyl derivatives in the gaseous state: Part 4. Barrier of internal rotation in biphenyl, perdeuterated biphenyl and seven non-ortho-substituted halogen derivatives. *J. Mol. Struct.* **1985**, *128*, 115–125.
- (42) Haaland, A.; Shorokhov, J. D.; Tverdova, N. V. Topological analysis of electron densities: Is the presence of an atomic interaction line in an equilibrium geometry a sufficient condition for the existence of a chemical bond? *Chem.–Eur. J.* **2004**, *10*, 4416–4421.
- (43) Strenalyuk, T.; Haaland, A. Chemical bonding in the inclusion complex of He in adamantane (He@adam): The origin of the barrier to dissociation. *Chem.–Eur. J.* **2008**, *14*, 10223–10226.
- (44) von Hopffgarten, M.; Frenking, G. Chemical bonding in the inclusion complex of He in adamantane, He@adam: Antithesis and complement. *Chem.–Eur. J.* **2008**, *14*, 10227–10233.
- (45) Krapp, A.; Frenking, G. Is this a chemical bond? A theoretical study of Ng<sub>2</sub>@C<sub>60</sub> (Ng=He, Ne, Ar, Kr, Xe). *Chem.–Eur. J.* **2007**, *13*, 8256–8270.
- (46) Weinhold, F. Natural bond critical point analysis: quantitative relationships between natural bond orbital-based and QTAIM-based topological descriptors of chemical bonding. *J. Comput. Chem.* **2012**, *33*, 2440–2449.
- (47) Cukrowski, I.; de Lange, J. H.; Adeyinka, A. S.; Mangondo, P. Evaluating common QTAIM and NCI interpretations of the electron density concentration through IQA interaction energies and 1D cross-sections of the electron and deformation density distributions. *Comput. Theor. Chem.* **2015**, *1053*, 60–76.
- (48) Matta, C. F.; Sadjadi, S-A.; Braden, D. A.; Frenking, G. The barrier to the methyl rotation in *cis*-2-butene and its isomerization energy to *trans*-2-butene, revisited. *J. Comput. Chem.* **2016**, *37*, 143–154.
- (49) Grimme, S.; Mück-Lichtenfeld, C.; Erker, G.; Kehr, G.; Wang, H.; Beckers, H.; Willner, H. When do interacting atoms form a chemical bond? Spectroscopic measurements and theoretical analyses of dideuteriophenanthrene. *Angew. Chem. Int. Ed.* **2009**, *48*, 2592–2595.

(50) de Lange, J. H.; van Niekerk, D. M. E.; Cukrowski, I. Quantifying individual (anti)bonding molecular orbitals' contributions to chemical bonding. *Phys. Chem. Chem. Phys.* **2019**, *21*, 20988–20998.

(51) de Lange, J. H.; van Niekerk, D. M. E.; Cukrowski, I. FALDI-based criterion for and the origin of an electron density bridge with an associated (3,-1) critical point on Bader's molecular graph, *J. Comp. Chem.* **2018**, *39*, 2283–2299.

(52) Frisch, M. J.; Trucks, G. W.; Schlegel, H. B.; Scuseria, G. E.; Robb, M. A.; Cheeseman, J. R.; Scalmani, G.; Barone, V.; Mennucci, B.; Petersson, G. A. et al. *Gaussian 09*, Revision D.01; Gaussian, Inc.: Wallingford, CT, 2013.

(53) Grimme, S. Density functional theory with London dispersion corrections. *Wiley Interdiscip. Rev. Comput. Mol. Sci.* **2011**, *1*, 211–228.

(54) AIMAll (Version 19.02.13), Keith, T. A. TK Gristmill Software, Overland Park KS, USA, 2019 (aim.tkgristmill.com).

(55) Ruedenberg, K.; Schmidt, M. W. Physical understanding through variational reasoning: Electron sharing and covalent bonding. *J. Phys. Chem. A* **2009**, *113*, 1954–1968.

(56) Tognetti, V.; Joubert, L. On the physical role of exchange in the formation of an intramolecular bond path between two electronegative atoms. *J. Chem. Phys.* **2013**, *138*, 024102–024110.

(57) Jabłonski, M. On the uselessness of Bond Paths linking distant atoms and on the violation of the concept of privileged exchange channels, *ChemistryOpen* **2019**, *8*, 497–507.

(58) de Lange, J. H.; van Niekerk, D. M. E.; Cukrowski, I. FALDI-based decomposition of an atomic interaction line leads to 3D representation of the multicentre nature of interactions, *J. Comp. Chem.* **2018**, *39*, 973–985.

# TOC Graphic

